AIP | Applied Physics Letters

Distance-dependent energy transfer between CdSe/CdS quantum dots and a two-dimensional semiconductor

Kenneth M. Goodfellow, Chitraleema Chakraborty, Kelly Sowers, Pradeep Waduge, Meni Wanunu, Todd Krauss, Kristina Driscoll, and A. Nick Vamivakas

Citation: Applied Physics Letters **108**, 021101 (2016); doi: 10.1063/1.4939845
View online: http://dx.doi.org/10.1063/1.4939845
View Table of Contents: http://scitation.aip.org/content/aip/journal/apl/108/2?ver=pdfcov
Published by the AIP Publishing

Distance-dependent energy transfer between CdSe/CdS quantum dots and a two-dimensional semiconductor

Kenneth M. Goodfellow,[1] Chitraleema Chakraborty,[2] Kelly Sowers,[3] Pradeep Waduge,[4] Meni Wanunu,[4] Todd Krauss,[1,3] Kristina Driscoll,[5] and A. Nick Vamivakas[1,a)]
[1]*Institute of Optics, University of Rochester, Rochester, New York 14627, USA*
[2]*Materials Science, University of Rochester, Rochester, New York 14627, USA*
[3]*Department of Chemistry, University of Rochester, Rochester, New York 14627, USA*
[4]*Department of Physics, Northeastern University, Boston, Massachusetts 02115, USA*
[5]*Department of Physics, Rochester Institute of Technology, Rochester, New York 14627, USA*

(Received 20 September 2015; accepted 28 December 2015; published online 11 January 2016)

Atomically thin semiconductors, such as the transition metal dichalcogenides, show great potential for nanoscale photodetection, energy harvesting, and nanophotonics. Here, we investigate the efficiency of energy transfer between colloidal quantum dots with a cadmium selenide core and cadmium sulfide shell and monolayer molybdenum diselenide ($MoSe_2$). We show that $MoSe_2$ effectively quenches the fluorescence of quantum dots when the two materials are in contact. We then separate the $MoSe_2$ and quantum dots by inserting variable thickness hexagonal boron nitride (h-BN) spacers and show that the efficiency at which the $MoSe_2$ quenches fluorescence decreases as the h-BN thickness is increased. For distances d, this trend can be modeled by a $1/d^4$ decay, in agreement with theory and recent studies involving graphene. © *2016 AIP Publishing LLC*. [http://dx.doi.org/10.1063/1.4939845]

Compelled by the isolation of graphene,[1] recent years have brought upon intense studies of atomically thin materials. Graphene's lack of an intrinsic bandgap limits its usefulness in transitive and logical applications. Fortunately, other materials that can be made atomically thin do have a bandgap; hexagonal boron nitride (h-BN) demonstrates strong dielectric and insulating properties,[2,3] whereas the monolayer transition metal dichalcogenides (TMDCs) have bandgaps in the 1.7–2 eV range.[4,5] The family of TMDCs, such as molybdenum disulfide (MoS_2), being photoluminescent at monolayer thickness[4,6] and electroluminescent,[7] has been shown to have utility for nanophotonic devices.[8–14]

Of greater interest is the ability to couple these atomically thin materials to various nanostructures in order to enhance the abilities of integrated nanosystems.[15,16] Graphene has been shown to produce strong fluorescence quenching of zero-dimensional semiconductor nanocrytals [quantum dots (QDs)],[17–19] demonstrating energy transfer from the QDs to the graphene and exemplifying ability for energy collection and photodetection. In addition, MoS_2 has been recently coupled to QDs[20,21] and silver nanowires,[22] justifying the pursuit of atomically thin semiconductors for light collection and nanoplasmonics, as well as for studies of energy transfer mechanisms with these hybrid nanostructures. QDs are particularly interesting for these types of hybrid devices, as their size can be tailored to absorb and emit across a broad spectrum,[23] paving the way for a next generation of photodetectors and photovoltaic devices.

In this letter, we study the energy transfer between core/shell cadmium selenide/cadmium sulfide (CdSe/CdS) colloidal QDs and monolayer molybdenum diselenide ($MoSe_2$). We first demonstrate that $MoSe_2$ effectively quenches QD fluorescence when the two materials are brought into contact and the QDs are excited with laser light. We then investigate the distance dependence of the energy transfer to the $MoSe_2$ by placing nanosheets of h-BN between the $MoSe_2$ and QDs. This atomically thin spacer of h-BN provides enough screening to reduce the quenching efficiency of the $MoSe_2$. By studying several of these heterostructures with varying thicknesses of h-BN, we find that the energy transfer can be modeled to a $1/d^4$ dependence, where d is the total distance between the center of the QD and the $MoSe_2$. This model also agrees with graphene/QD systems, which demonstrate Förster resonant energy transfer (FRET) mechanisms.[17–19,24,25]

A schematic of our experiment is shown in Fig. 1(a). A dilute solution of CdSe/CdS quantum dots was spun onto a clean glass coverslip. A viscoelastic stamp dry transfer technique[26] was then used to deposit h-BN or monolayer $MoSe_2$ onto the QD sample (see supplementary material for more details[27]). Varying thicknesses of h-BN (d_{BN}) were used to separate the $MoSe_2$ and QDs. The h-BN thickness was determined by atomic force microscopy (AFM). The approximate size of the QD radius (z_0) used was determined by transmission electron microscopy (TEM), as shown in Fig. 1(b). (See supplementary Figure S1 for a statistical distribution of sizes of measured defects.[27])

Figure 1(c) shows the emission spectrum of a representative QD as well as the differential reflectance $\triangle R/R = (R_{flake} - R_{glass})/R_{glass}$ of $MoSe_2$, which is proportional to the absorption spectrum. The differential reflectance was measured for a single-layer $MoSe_2$ sample on a glass coverslip using a white light source directed through a spatial filter and to a microscope objective (numerical aperture = 0.75) in an inverted microscope setup. The reflected light was directed to a spectrometer with a charge coupled device (CCD) camera, and the differential reflectance was calculated from spectra taken on the flake and on the glass. The specific QD presented has a peak of emission at around 620 nm, but QDs were observed to have emission ranging from about 590 nm to 640 nm, depending on the specific dot.

a)nick.vamivakas@rochester.edu

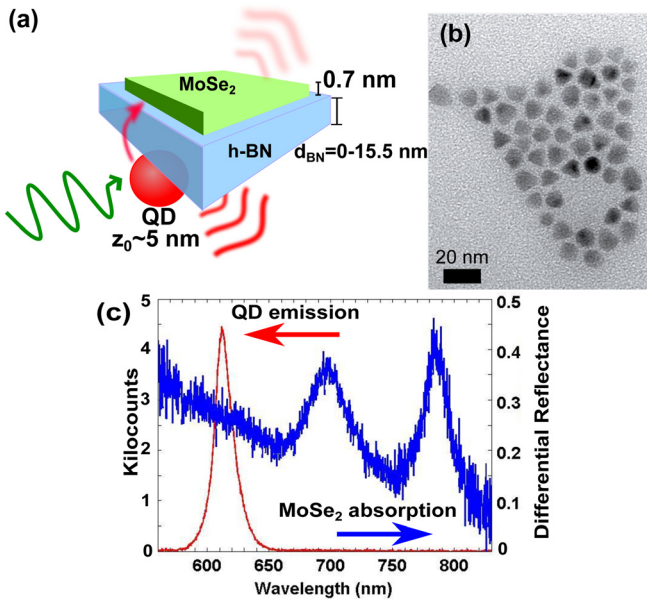

FIG. 1. (a) Schematic of $MoSe_2$/QD structure. (b) TEM image of the QDs used in the study. (c) Emission spectrum for a typical QD and differential reflectance for $MoSe_2$. For the QD, excitation wavelength = 532 nm, and power = 650 nW.

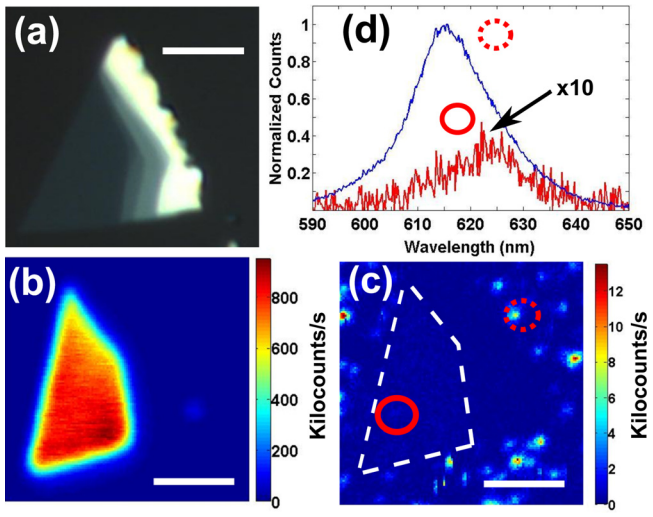

FIG. 2. (a) Microscope image of the $MoSe_2$/QD structure studied. (b) and (c) Fluorescence images of the sample from Fig. 2(a) taken with a 555 nm longpass filter (b) or additional 650 nm shortpass and 645/180 nm bandpass filters (c) in front of the APD. The dotted line in (c) represents the monolayer flake. The circles correspond to QDs measured in (d). For (a)–(c), scale bars = 5 μm. (d) Spectra from QDs located off of the flake (dotted circle) and under the $MoSe_2$ (solid line circle). For all panels, excitation wavelength = 532 nm, and power = 650 nW.

Nevertheless, this region is safely in the region of high, fairly flat absorption for $MoSe_2$. Other TMDCs have attractive absorption characteristics for our experiment,[28] but we chose $MoSe_2$ as our atomically thin semiconductor. The family of TMDCs is highly photoluminescent at single layer thickness due to the transition from an indirect to a direct bandgap. The two direct bandgap transitions, the A and B excitons, are brought about due to strong valence band spin-orbit coupling. For $MoSe_2$, the A and B excitons recombine and emit light at 790 nm and 700 nm,[5] respectively, whereas other TMDCs have emission that is spectrally close to the QD emission.[6,29] Thus, the choice of $MoSe_2$ mitigates any confounding emission effects between the atomically thin semiconductor and the QDs.

We first study the effects of depositing the $MoSe_2$ directly onto the QDs with no h-BN spacer. The samples were placed onto a home-built inverted microscope set-up equipped with an air objective. A laser ($\lambda = 532$ nm) was directed to the sample, and the sample was raster scanned using a nanopositioning stage (Mad City Labs, Inc.). The resulting fluorescence was then directed to either an avalanche photodiode (APD) to create fluorescence images or to a spectrometer equipped with a CCD camera. To monitor all fluorescence at the APD, only a 555 nm long pass filter was used to cut out the laser line. Figure 2(a) shows an optical micrograph of the $MoSe_2$/QD sample studied. Figure 2(b) displays a fluorescence image of the sample. The dominant feature in this scan is the photoluminescence (PL) from the $MoSe_2$, and the PL spectrum confirms monolayer thickness (see Figure S2).[27] In order to see the effect of the $MoSe_2$ on the QDs, we placed a shortpass filter with a cut-off wavelength of 650 nm and a bandpass filter centered at 645 nm with 90 nm of transmission above and below (645/180 nm) to block the $MoSe_2$ signal in front of the APD. The resulting fluorescence image is shown in Fig. 2(c). The much weaker fluorescence from the QDs can now be observed. What is apparent is the lack of QD fluorescence from the monolayer $MoSe_2$ flake region (dashed box), implying that the $MoSe_2$ is quenching the QD emission. Due to the homogeneity of dispersion of QDs on the substrate, if there was no quenching mechanism, QD fluorescence would be expected in the entire scanning area. We investigate the spectral emission of QDs under and off of the flake in Fig. 2(d), showing spectra from one QD off of the flake and one QD under with locations specified in Fig. 2(c). A clear reduction in spectral intensity is demonstrated for the QD under the flake. The peak spectral emission variation in the QDs is present in the absence of the $MoSe_2$. This is due to the inhomogeneous size distribution, and it is common for PL from single QDs to have peaks that cover the ensemble PL spectrum. To quantify the effect of the QD fluorescence quenching, we define the quenching efficiency (QE) to be $QE = 1 - I_{on}/I_{off}$, where I_{on} (I_{off}) is the integrated fluorescence intensity of a QD on (off) the $MoSe_2$ flake. Based on QDs on and off the flake, we find a QE of 0.94 for this sample. The QDs measured for this value were single QDs and not clusters; see the supplementary material and Fig. S3 for a discussion on this point.[27]

We are now in a position to investigate the effect of separating the QDs and $MoSe_2$. Because h-BN is a large bandgap (~6 eV) semiconductor,[2] it will not absorb the fluorescence from the $MoSe_2$ or the QDs and can serve as a dielectric spacer. The thicknesses of the h-BN were between approximately 3.6 nm and 15.5 nm thick, as determined by AFM. Figure 3(a) shows a wide-field microscope image of our sample. In Fig. 3(a), the $MoSe_2$ resides on a flake of h-BN that is ~3.6 nm thick as measured by AFM (Fig. 3(a) inset). Due to the large bandgap of the h-BN, the thin h-BN flake is nearly invisible and has poor contrast from the substrate. (See Figures S4 and S5 for data of samples with thicker h-BN.[27]) Figure 3(b) displays a fluorescence image of the sample with only the 555 nm longpass filter in front of the APD, which shows primarily $MoSe_2$ fluorescence.

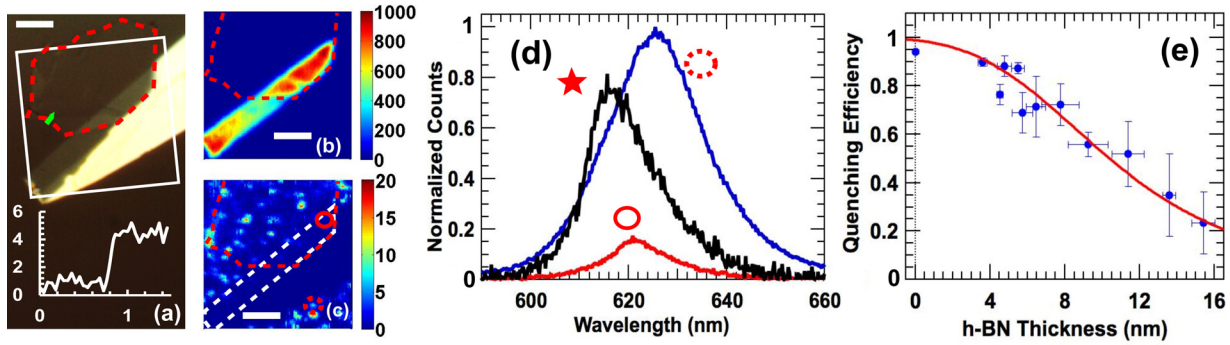

FIG. 3. (a) Optical micrograph of an h-BN/$MoSe_2$/QD structure. The h-BN is ~3.6 nm thick. Inset: Line cut as measured by AFM of the height (nm) as a function of distance (μm) in the direction of the green arrow. (b) and (c) Fluorescence images of the sample from Fig. 3(a) taken with a 555 nm longpass filter (b) or additional 650 nm shortpass and 645/180 nm bandpass filters (c) in front of the APD. Units for the colorbar are kilocounts/second. In (a)–(c), the red dotted lines outline the h-BN flake, while in (c), the white line outlines the monolayer $MoSe_2$ flake. The circles correspond to QDs measured in (d). Scale bars = 5 μm. (d) Spectra from QDs located off of the flakes (dotted circle) and under the h-BN and $MoSe_2$ (solid line circle). The star notates the spectrum from a QD under $MoSe_2$ and flake of h-BN ~14 nm thick. For (b)–(d), excitation wavelength = 532 nm, and power = 650 nW. (e) Plot of the quenching efficiency of the $MoSe_2$ as a function of the thickness of the h-BN. The line, fit for a value for z_0 (QD radius) of 5 nm as measured by TEM, utilizes an energy transfer model based upon a $1/d^4$ decay of quenching efficiency, where d is the total distance between the center of the QD to the $MoSe_2$.

However, differences become apparent when the scan is performed again with the 650 nm shortpass and 645/180 nm bandpass filter placed in front of the APD, as shown in Fig. 3(c). Areas of weaker signal coming from QDs located underneath the $MoSe_2$ are apparent in this image. Although the fluorescence is much weaker compared to the QDs off of the flake, the observed signal from the QDs under the flake in this sample is stronger than that observed for the sample with no h-BN in Fig. 2(c). Thus, the h-BN reduces the fluorescence quenching of the QDs by the $MoSe_2$. Figure 3(d) displays the spectra of two QDs from this sample, one under the $MoSe_2$ and the h-BN and one off of the flakes. In addition, this figure displays the spectrum of a QD under $MoSe_2$ and a thicker (approximately 14 nm) flake of h-BN, as noted by the star. As expected, the spectral intensity for the QD under the $MoSe_2$ from the thicker h-BN sample is stronger than the one from the thinner h-BN sample, but both are still stronger than the intensity from the QD under $MoSe_2$ without h-BN, as shown in Fig. 2(d). The QE for the sample presented in Fig. 3(a) was measured to be 0.9, whereas the QE for the sample with ~14 nm of h-BN was 0.35, implying a decrease in QE as the h-BN thickness increases.

Finally, we investigate the nature of the energy transfer by measuring samples of varying thicknesses of h-BN. Figure 3(e) presents the QE of the $MoSe_2$ for each of the samples measured as a function of the h-BN thickness. For each sample, the QE was calculated for 3 to 8 QDs under the $MoSe_2$. Clearly, there is a steady decrease in the QE as the h-BN spacer thickness increases. We model the energy transfer mechanism similarly to models for graphene and nanostructures, predicting an increase in nonradiative decay rate, and hence an increase in quenching, with decreasing separation.[17–19,30] The model that we use predicts a quenching efficiency given by

$$QE = 1 - \left(1 \Big/ \left(1 + \left(\frac{d_0}{d_{BN} + z_0}\right)^n\right)\right), \qquad (1)$$

where d_{BN} is the thickness of the h-BN, z_0 is the minimal distance between the center of the QD and the $MoSe_2$ in the absence of the h-BN, d_0 is the effective Förster radius (the distance at which the efficiency of energy transfer falls to 50%), and n is a number related to the dimensionality of the donor and acceptor. Note that the total distance between the center of the QD and the $MoSe_2$, d, is given by $d = d_{BN} + z_0$. Based on Förster energy transfer theory, the dimensionality factor should be $n = 6$ for the energy transfer between two point-like dipoles, $n = 5$ for a line of dipoles as the acceptor, $n = 4$ for a sheet of dipoles, and $n = 3$ for transfer to a bulk material.[31] This mechanism has been studied for energy transfer from point-like dipoles to one-dimensional materials such as carbon nanotubes and nanowires,[32–34] and previous reports of energy transfer from QDs to graphene[17–19] successfully modeled the increasing exciton lifetime with increasing QD/graphene thickness to an $n = 4$ model. The main difference between our model and previous work using graphene is that we are modeling intensity quenching instead of lifetime quenching.

Based on Equation (1), we fit the data assuming a value of $z_0 = 5$ nm as measured by TEM. A value of $n = 4$ yields a value of $d_0 = 15.4$ nm for $z_0 = 5$. This value for the effective Förster radius is reasonable, and the model fits well for most h-BN spacers. The discrepancy at some smaller values of thickness may be due to the strong anisotropy of $MoSe_2$. Excitons in TMDCs have excitons oriented strongly in-plane,[35] whereas the dipole orientation of the QDs are randomly oriented. The effect in the difference in dipole orientation between the QD and $MoSe_2$ will be accentuated at smaller distances. In addition, the electron in the QD is in the shell while the hole is confined to the core; thus, despite the physical separation caused by the h-BN, the exciton is approximately confined to the core. As a result, at smaller h-BN thicknesses comparable to the shell thickness, QE differs from what is predicted by theory. To further confirm that our quenching theory is not affected by factors such as the inhomogenous dielectric environment, finite difference time domain (FDTD) simulations confirmed that the far-field emission pattern of the QD is not affected significantly by the addition of a multilayer h-BN sheet.

In summary, we have demonstrated distance dependent energy transfer mechanisms between semiconductor nanocrystals

and monolayer $MoSe_2$. When brought into direct contact, the $MoSe_2$ exhibits a quenching efficiency of around 94% of the QD fluorescence, but this efficiency could be decreased by inserting thin layers of insulating h-BN. A natural next step is to control the atomically thin semiconductor electrically by applying metal contacts to control the absorption of the QD emission, similar to experiments performed on graphene.[16] The possibility of controlling properties such as refractive index and absorption electrically[36] will guide the way towards control of nanoscale energy transfer, which will steer to a path of next-generation optoelectronic devices.

We acknowledge Tanya Malhotra for assistance with FDTD simulations. The authors acknowledge support from the Institute of Optics at the University of Rochester, the National Science Foundation (Grant Nos. EFMA-1542707 and CHE-1307254), and Air Force Office of Scientific Research (FA9550-16-1-0020).

[1]K. S. Novoselov, D. Jiang, F. Schedin, T. J. Booth, V. V. Khotkevich, S. V. Morozov, and A. K. Geim, Proc. Natl. Acad. Sci. USA **102**, 10451 (2005).
[2]C. R. Dean, A. F. Young, I. Meric, C. Lee, L. Wang, S. Sorgenfrei, K. Watanabe, T. Taniguchi, P. Kim, K. L. Shepard, and J. Hone, Nat. Nanotechnol. **5**, 722 (2010).
[3]D. Golberg, Y. Bando, Y. Huang, T. Terao, M. Mitome, C. Tang, and C. Zhi, ACS Nano **4**, 2979 (2010).
[4]K. F. Mak, C. Lee, J. Hone, J. Shan, and T. F. Heinz, Phys. Rev. Lett. **105**, 136805 (2010).
[5]P. Tonndorf, R. Schmidt, P. Böttger, X. Zhang, J. Börner, A. Liebig, M. Albrecht, C. Kloc, O. Gordan, D. R. T. Zahn, S. M. de Vasconcellos, and R. Bratschitsch, Opt. Express **21**, 4908 (2013).
[6]A. Splendiani, L. Sun, Y. Zhang, T. Li, J. Kim, C.-Y. Chim, G. Galli, and F. Wang, Nano Lett. **10**, 1271 (2010).
[7]R. S. Sundaram, M. Engel, A. Lombardo, R. Krupke, A. C. Ferrari, P. Avouris, and M. Steiner, Nano Lett. **13**, 1416 (2013).
[8]Z. Yin, H. Li, H. Li, L. Jiang, Y. Shi, Y. Sun, G. Lu, Q. Zhang, X. Chen, and H. Zhang, ACS Nano **6**, 74 (2012).
[9]O. Lopez-Sanchez, D. Lembke, M. Kayci, A. Radenovic, and A. Kis, Nat. Nanotechnol. **8**, 497 (2013).
[10]B. Radisavljevic, A. Radenovic, J. Brivio, V. Giacometti, and A. Kis, Nat. Nanotechnol. **6**, 147 (2011).
[11]R. Cheng, D. Li, H. Zhou, C. Wang, A. Yin, S. Jiang, Y. Liu, Y. Chen, Y. Huang, and X. Duan, Nano Lett. **14**, 5590 (2014).
[12]J. S. Ross, P. Klement, A. M. Jones, N. J. Ghimire, J. Yan, D. G. Mandrus, T. Taniguchi, K. Watanabe, K. Kitamura, W. Yao, D. H. Cobden, and X. Xu, Nat. Nanotechnol. **9**, 268 (2014).
[13]C. Chakraborty, L. Kinnischtzke, K. M. Goodfellow, R. Beams, and A. N. Vamivakas, Nat. Nanotechnol. **10**, 507 (2015).
[14]K. M. Goodfellow, C. Chakraborty, R. Beams, L. Novotny, and A. N. Vamivakas, Nano Lett. **15**, 5477–5481 (2015).
[15]G. Konstantatos, M. Badioli, L. Gaudreau, J. Osmond, M. Bernechea, F. P. G. de Arquer, F. Gatti, and F. H. L. Koppens, Nat. Nanotechnol. **7**, 363 (2012).
[16]J. Lee, W. Bao, L. Ju, P. J. Schuck, F. Wang, and A. Weber-Bargioni, Nano Lett. **14**, 7115 (2014).
[17]L. Gaudreau, K. J. Tielrooij, G. E. D. K. Prawiroatmodjo, J. Osmond, F. J. G. de Abajo, and F. H. L. Koppens, Nano Lett. **13**, 2030 (2013).
[18]F. Federspiel, G. Froehlicher, M. Nasilowski, S. Pedetti, A. Mahmood, B. Doudin, S. Park, J.-O. Lee, D. Halley, B. Dubertret, P. Gilliot, and S. Berciaud, Nano Lett. **15**, 1252 (2015).
[19]Z. Chen, S. Berciaud, C. Nuckolls, T. F. Heinz, and L. E. Brus, ACS Nano **4**, 2964 (2010).
[20]F. Prins, A. J. Goodman, and W. A. Tisdale, Nano Lett. **14**, 6087 (2014).
[21]D. Kufer, I. Nikitskiy, T. Lasanta, G. Navickaite, F. H. L. Koppens, and G. Konstantatos, Adv. Mater. **27**, 176 (2015).
[22]K. M. Goodfellow, R. Beams, C. Chakraborty, L. Novotny, and A. N. Vamivakas, Optica **1**, 149 (2014).
[23]L. E. Brus, J. Chem. Phys. **80**, 4403 (1984).
[24]K. J. Tielrooij, L. Orona, A. Ferrier, M. Badioli, G. Navickaite, S. Coop, S. Nanot, B. Kalinic, T. Cesca, L. Gaudreau, Q. Ma, A. Centeno, A. Pesquera, A. Zurutuza, H. de Riedmatten, P. Goldner, F. J. G. de Abajo, P. Jarillo-Herrero, and F. H. L. Koppens, Nat. Phys. **11**, 281 (2015).
[25]R. S. Swathi and K. L. Sebastian, J. Chem. Phys. **130**, 086101 (2009).
[26]A. Castellanos-Gomez, M. Buscema, R. Molenaar, V. Singh, L. Janssen, H. S. J. van der Zant, and G. A. Steele, 2D Mater. **1**, 011002 (2014).
[27]See supplementary material at http://dx.doi.org/10.1063/1.4939845 for sample preparation, $MoSe_2$ PL, analysis of QDs, and data from thicker samples.
[28]Y. Li, A. Chernikov, X. Zhang, A. Rigosi, H. M. Hill, A. M. van der Zande, D. A. Chenet, E.-M. Shih, J. Hone, and T. F. Heinz, Phys. Rev. B **90**, 205422 (2014).
[29]W. Zhao, Z. Ghorannevis, L. Chu, M. Toh, C. Kloc, P.-H. Tan, and G. Eda, ACS Nano **7**, 791 (2013).
[30]Y.-J. Yu, K. S. Kim, J. Nam, S. R. Kwon, H. Byun, K. Lee, J.-H. Ryou, R. D. Dupuis, J. Kim, G. Ahn, S. Ryu, M.-Y. Ryu, and J. S. Kim, Nano Lett. **15**, 896 (2015).
[31]W. L. Barnes, J. Mod. Opt. **45**, 661 (1998).
[32]P. L. Hernández-Martínez and A. O. Govorov, Phys. Rev. B **78**, 035314 (2008).
[33]I. V. Bondarev, G. Y. Slepyan, and S. A. Maksimenko, Phys. Rev. Lett. **89**, 115504 (2002).
[34]E. Shafran, B. D. Mangum, and J. M. Gerton, Nano Lett. **10**, 4049 (2010).
[35]J. A. Schuller, S. Karaveli, T. Schiros, K. He, S. Yang, I. Kymissis, J. Shan, and R. Zia, Nat. Nanotechnol. **8**, 271 (2013).
[36]E. J. G. Santos and E. Kaxiras, ACS Nano **7**, 10741 (2013).